communications earth & environment

ARTICLE

https://doi.org/10.1038/s43247-023-00804-7 OPEN

Estimating coastal flood damage costs to transit infrastructure under future sea level rise

Michael V. Martello [1]✉ & Andrew J. Whittle[1]

Future sea level rise (SLR) and associated increases in the frequency and intensity of coastal flooding poses significant threats to coastal communities and transit systems. Yet current literature and practice lack methods for estimating flood damage costs to transit systems. Here, we construct an event-specific flood damage cost estimation framework for transit systems, simulating separately flood ingress into underground spaces. We apply this framework to the MBTA rail transit system in Boston, estimating damages under several coastal flood events with SLR and project expected annualized losses (EAL) through 2100 with uncertain SLR. We estimate EALs to the MBTA system have doubled since 2008 to $24.4 M/year and are expected to reach $58 M/year by 2030 under all SLR scenarios. Our results suggest that absent adaptation schemes, particularly at tunnel ingress locations, coastal flood risk will continue to accelerate, potentially resulting in permanent inundation of underground and low-lying sections of the transit system.

[1] Department of Civil & Environmental Engineering, Massachusetts Institute of Technology, 77 Massachusetts Avenue, Cambridge, MA, USA.
✉email: martello@mit.edu

Climate change and sea level rise (SLR) are expected to increase the frequency and severity of coastal flood events, posing a wide array of technical, social, economic, and scientific challenges[1,2]. Absent any mitigation measures, increases in exposure to these hazards will result in higher risks and greater consequences of flooding[3,4]. Much like any other public or private sector investment, motivating investment in such flood risk reduction requires a demonstration that the benefits (i.e., of avoiding future flood-related damages) outweighs the costs (of design, construction, and maintenance). Quantifying the coastal flood risk reduction benefits of a given project in monetary terms requires the assessment of flood damage costs for the full range of potential coastal flood events against which a given project is expected to provide protection.

While there exists a well-established base of literature and practice focused on estimating the damage costs of flood events for commercial and residential buildings for both public[3,5–9] and private sector applications[10,11], similar methodologies have yet to be extended to physical infrastructure assets. Despite decades of practice and research, existing flood damage cost estimation methods and resultant climate adaptation assessments routinely neglect flood risk reduction benefits to public infrastructures[9,12,13]. In urban areas, the consequences of damage to physical infrastructures are likely to represent a significant portion of direct damage costs. For example, regional infrastructure systems in the greater New York and New Jersey area sustained $17.1B in direct damages due to Hurricane Sandy in 2012, corresponding to 23% of the estimated $62.3B in overall direct damage costs, with an estimated $5B in direct damages to the New York City Transit (NYCT) system[14]. As sea levels continue to rise, infrastructure managers and planners will increasingly require better flood risk quantification methods to understand projected future risks and risk reduction benefits of capital investments in climate adaptation projects. While some prior studies include rather cursory estimates of flood risk reduction benefits to infrastructure, either via a percentage-multiplier based on limited case study data[15] or inclusion of infrastructure as a separate land use category[16], these methods do not adequately address the causal mechanisms characterizing the consequences of flood exposure for infrastructure assets or subsystems.

In the particular case of urban rail rapid transit systems, which are often located below-ground or transecting floodplains at-grade, an understanding of present and projected future flood risk not only requires a robust understanding of projected future coastal flood exposure, but also requires a detailed understanding of the associated infrastructure systems (e.g., power, signals, etc.), the physical arrangement of the stations, tunnels, and ventilation systems, as well as their relation to the built environment, particularly where water can flow into underground spaces[17,18]. While flood severity along at-grade portions of a transit system can be inferred directly from flood maps[19,20] or hydrodynamic simulations[21], the determination of flood severity in underground portions of the system is less straightforward. There are a variety of methods that have been proposed to evaluate flood exposure in underground spaces including: i) inference from the extent of flooding at the ground surface[21], ii) probabilistic estimation as a percentage of the overall tunnel network length[22], iii) approximation via a gravity-based heuristic (i.e., assuming water flows downhill through a tunnel network[18,23], or iv) estimation via expert assessment[24,25]. Flood extents can be simulated at higher fidelity (i.e., inclusive of estimated flood depths) via a hydraulic model, if sufficient information is available to characterize water inflow volumes over time[26–30]. Given these resulting flood extents, prior studies have primarily focused on characterizing tunnel safety during evacuation events[24,27], network performance via graph theoretic measures[18,21], or vulnerability as measured by various indices[23,29]. Though a small subset of the reviewed studies attempt to quantify monetary damages to rail transit infrastructure either based on the length of tunnel flooded[22] or via flood depth-informed damage categories[19,20], neither assessment method characterizes damage at the asset level, nor meaningfully considers sources of uncertainty in damage assessment. Further, none of the studies surveyed have employed a high-fidelity coupled hydrodynamic-hydraulic model to inform a flood damage cost estimation model.

Addressing this gap in the literature, we develop an asset-level damage cost estimation model for rail rapid transit infrastructure, by estimating the flood extent and severity via the coupling of a previously established hydrodynamic coastal flood risk model[31] with a time-dependent hydraulic model of the underground portions of a transit network. Here, we estimate the extent and associated damage cost of coastal flooding across the MBTA rail rapid transit network in Boston (configuration as of 2021; Fig. 1) for a set of coastal flood events under a baseline sea level and several projected future SLR conditions. Using these systemwide flood projections, we use asset-level replacement cost estimates and transit-specific relationships between flood depth and damage severity[32], to estimate flood-related damages via a novel implementation of the unit loss method[6,33]. Our analyses incorporate uncertainties in flood depth estimates[34], asset replacement values (via an uncertain contingency estimate calibrated to real-world cost escalation data[35], and depth-damage functions[36] via Monte Carlo simulation. Using the resulting event-specific coastal flood damage estimates, we assess the full range of expected annualized losses (EAL) for the MBTA rail rapid transit system, characterizing the relationship between EAL and SLR. Given this relationship and the latest available SLR projections[1,37–39], we then develop estimates of EAL over time for the MBTA rail rapid transit system through the end of the 21st century.

Results

Using available data from the Massachusetts Coastal Flood Risk Model (MC-FRM), we assessed coastal flood risk for the MBTA rail rapid transit system considering flood events of varying return periods (1-in-2-year, 1-in-10-year, 1-in-20-year, 1-in-100-year, 1-in-1,000-year) across four sea level rise (SLR) regimes (+0.07 m, +0.43 m, +0.79 m, +1.34 m) measured relative to a 2000 baseline (1991–2009 tidal epoch). Figure 1 provides a representative sample of regional flood severity, systemwide tunnel inflow volumes, and flood depths under a 1-in-100-year flood event (i.e., 1% coastal flood exceedance probability, CFEP) with +0.79 m of SLR. Here, we observe widespread flooding throughout Greater Boston, with inundation along the entirety of the Blue Line, significant portions of the Orange, Red, and Silver Lines, and at critical rail maintenance facilities along the Orange, Blue, and Red Lines. The results in Fig. 1, show widespread flooding along the at-grade portions of the system with significant volumes of inflow into underground portions of the system, primarily through tunnel portals, that generate inflows one order of magnitude greater than other ingress pathways at transit stations (e.g., station entrances, ventilation shafts, etc.). The analyses show widespread flooding throughout the underground portions of the system in Downtown Boston, due to the interconnected nature of the underground space that allows floodwaters to inundate adjacent lines in the system (e.g., the Red Line in the sample event shown). Here, we expect flood depths exceeding 5 m along the majority of the Red, Orange, Blue, and Silver Line tunnels reaching to the crown of the running tunnels. At this level of saltwater inundation, we expect most linear assets

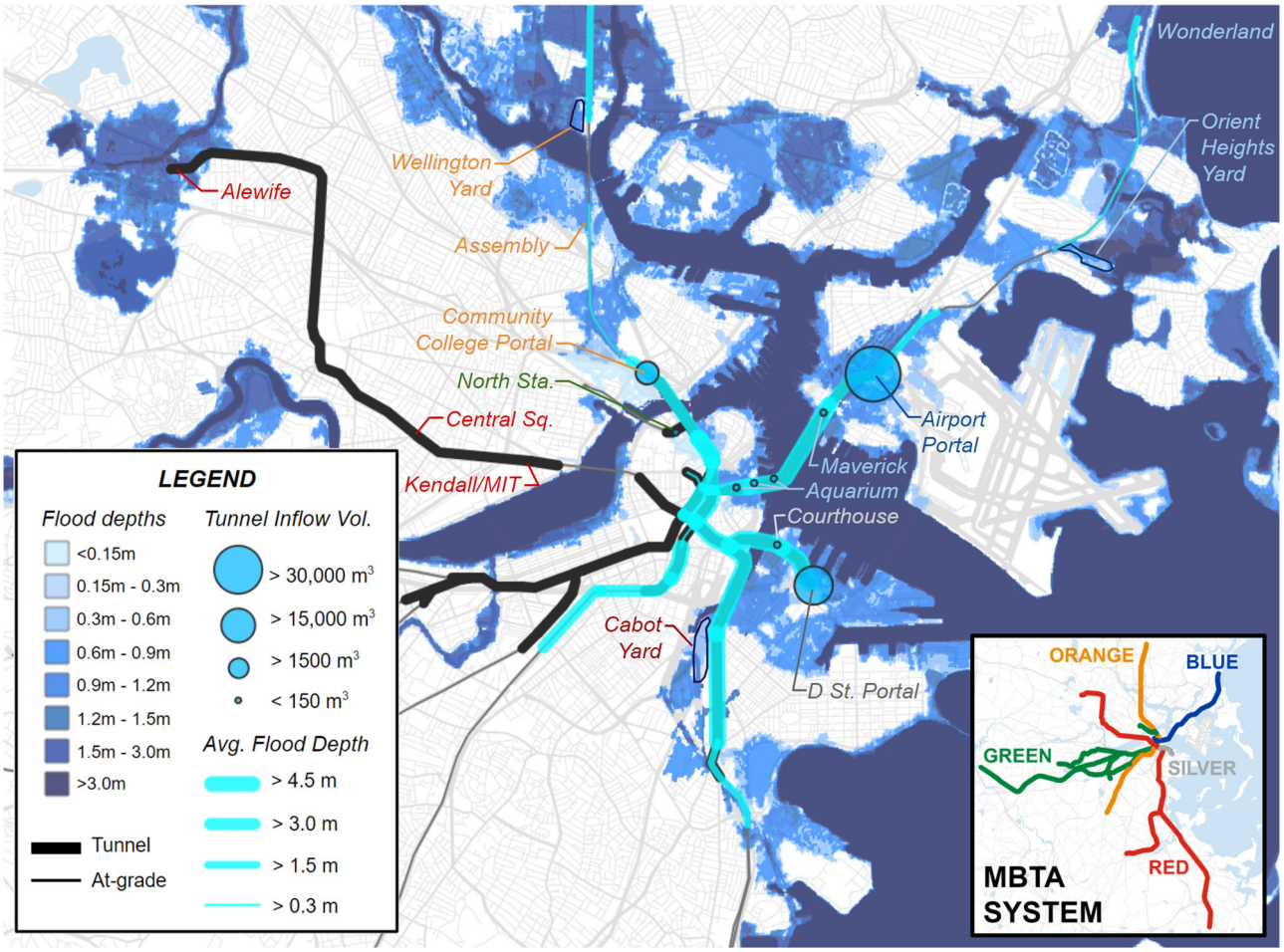

Fig. 1 Projected tunnel inflow volumes and flood depths across the MBTA rail rapid transit system under a 1-in-100-year (1% CFEP) coastal flood event with +0.79 m of SLR. At grade flood extents and depths (shown in a blue stepwise gradient) are overlain by average flood depths along rail rapid transit system segments (fluorescent blue) and tunnel inflow volumes (sky blue with black outline). At grade portions of the rail transit system are shown in thin black lines; underground (tunnel) portions are shown in thick black lines. Names of key locations in the system are shown in corresponding transit line color. Bottom right inset: overview of MBTA rail transit system (with corresponding line colors).

(i.e., rail, signals, power, lighting) and stations to sustain damages equivalent to at least 75% of replacement cost[32].

Considering the projected extent and severity of saltwater inundation across the entirety of the system, we estimate $5.3B (2020 USD) in direct flood damages to the MBTA rail rapid transit system, with expected losses of ~$1.2B to the Red, Blue, and Orange Lines, as shown in the probabilistic flood loss estimate shown in Fig. 2. We further observe that damage to connecting stations (i.e., stations where passengers can transfer) are expected to contribute $1.4B in flood losses, a greater proportion than any single line in isolation. We note the significant uncertainty in transit station replacement cost estimates largely informs uncertainty in station flood damage cost estimates, as well as uncertainty in overall flood damage estimates.

Figure 3 provides a summary of the probabilistic flood damage cost estimates for the MBTA rail rapid transit system across all assessed sea level conditions and flood severities (see Supplementary Fig. 1 for a summary of the underlying sample distributions and Supplementary Figs. 3–22 for corresponding inflows and flood extents). Here we find that estimated damage costs under the 1-in-20-year (5% CFEP) and 1-in-100-year (1% CFEP) coastal flood events are expected to increase by more than 10-fold compared to the baseline SLR (+0.07 m SLR), under even the most moderate SLR condition assessed (+0.43 m). Under future SLR, more frequent coastal flood events, notably the 1-in-2-year (50% CFEP), result in estimated damage costs that are significantly greater than those expected under comparatively less frequent coastal floods under the baseline SLR condition. Under 2008 baseline sea level conditions (+0.07 m of SLR) we expect flood losses of $24 M for a 1-in-20-year (5% CFEP) coastal flood event and $66 M in flood losses for a 1-in-100-year (1% CFEP) event. Even with a comparatively moderate SLR of +0.43 m (possible in Boston Harbor as soon as 2040 under the latest SSP5-8.5 SLR projections[1,37–39]) we expect significant increases in projected flood losses. For example, a 1-in-2-year (50% CFEP) coastal flood event is expected to cause $82 M in flood damage, which is greater than the losses expected in a 1-in-100-year flood event for the baseline sea level conditions. Considering flood risks under +1.34 m of SLR (possible in Boston Harbor as soon as 2075 under the latest SSP5-8.5 SLR projections[1,37–39]) we expect flood losses several orders of magnitude greater, with the same 1-in-2-year coastal flood event resulting in $5.4B in expected losses, suggesting permanent inundation of the entire Blue Line, as well as the interconnected underground portions of the network in Downtown Boston, with flood pathways via Aquarium Station on the Blue Line as well as via the tunnel portals along the Orange and Red Lines, all assuming there are no adaptation measures in place (Supplementary Fig. 18).

Estimating the expected annualized losses (EAL) to the MBTA rail rapid transit system, we observe a significant nonlinear

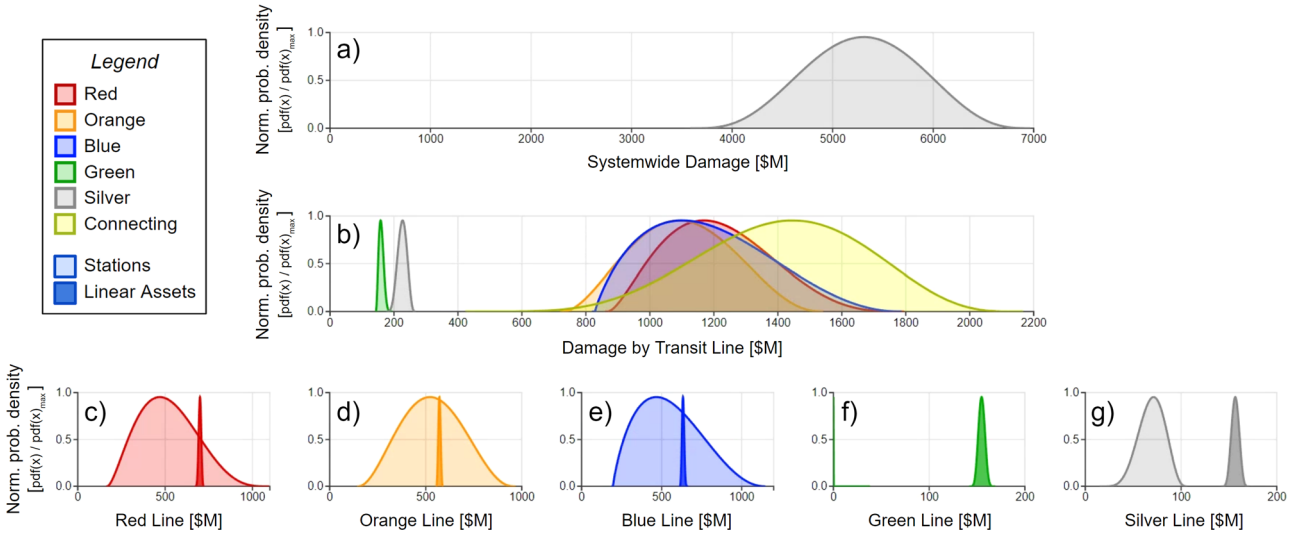

Fig. 2 Estimated flood losses to the MBTA rail rapid transit system under a 1-in-100-year (1% CFEP) coastal flood event with +0.79 m of SLR. **a** Probability density function (PDF) for overall systemwide damages (gray). **b** PDF for damage costs by transit line (colors corresponding to each line). **c**–**g** PDF for damage costs by asset type for each transit line (colors corresponding to each line). Lighter shaded PDF denotes damage costs to stations. Darker shaded PDF denotes damage costs to linear assets.

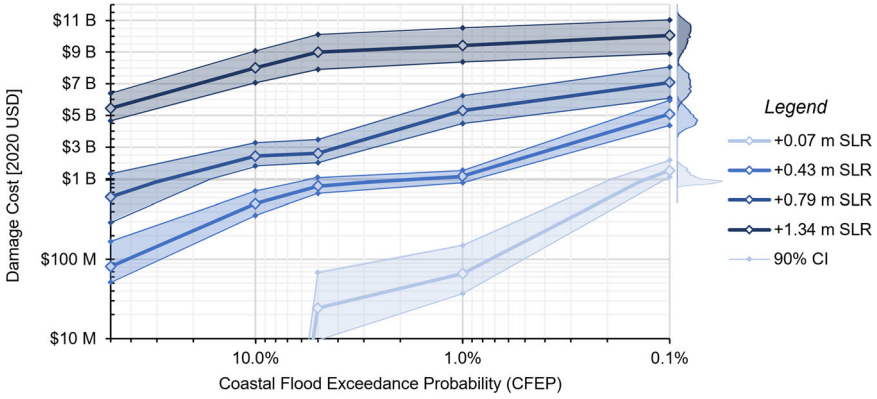

Fig. 3 Flood damage costs [2020 USD] vs. coastal flood exceedance probability (CFEP) under the four sea level rise (SLR) conditions assessed. Expected values (thick line) and 90% confidence interval (shaded region) of coastal flood damage costs under +0.07 m SLR (light blue), +0.43 m SLR (blue), +0.79 m SLR (dark blue), and +1.34 m SLR (navy blue). SLR values specified relative to a year 2000 baseline.

increase with respect to SLR (Fig. 4a). In fact, the sea level in Boston Harbor has already risen ~0.1 m above the 2000 baseline[40] such that the current EAL exposure of $24.4 M, already represents more than a 2-fold increase in exposure above 2008 baseline levels (EAL = $9.5 M). This increase is primarily driven by an expected increase in frequency of flooding along the Blue Line. As shown in Fig. 4b, relative to the mean value, we expect the range of EAL values (as described by the max and min values) to decrease with SLR, which has the practical effect of increasing the normality of the resulting generalized beta probability distributions (i.e., α and β converge) that describe EAL uncertainty, as shown in Fig. 4c, d.

Considering EAL over time for several uncertain SLR scenarios[1,37–39], as shown in Fig. 5, we expect EAL to increase by at least two orders of magnitude (i.e., 100×) across all SLR scenarios by 2100, though the 90% confidence interval also spans an order of magnitude across all scenarios. These results suggest that even under lowest warming scenario presented (i.e., SSP1-2.6), the MBTA could expect its coastal flood risk to reach ~$1.2B in EAL by 2100, a 49-fold increase compared to current levels. Under the worst case SLR scenario assessed (SSP5-8.5 low confidence projection), we expect EAL to reach $9.6B by 2100, absent any adaptation measures. Across all scenarios, we expect coastal flood risk to increase to ~$60 M in EAL by 2030, representing a 2.6-fold increase (i.e., 16% year-over-year growth) over current levels by the end of this decade. By 2050, EAL values range from ~$175 M (under SSP1-2.6 and SSP2-4.5 scenarios) to $200–$250 M (under the SSP5-8.5 and low confidence scenarios), representing a 7- to 10-fold increase above current levels. Beyond 2050, EAL estimates begin to diverge significantly depending on the SLR projection.

Discussion

These results suggest that the coastal flood risk of the MBTA rail rapid transit system has risen significantly in the past decade and is expected to compound at a 16% annual growth rate through the end of the decade, reaching an estimated $58 M in EAL by 2030 under all shared socioeconomic pathway (SSP) scenarios[1,37–39]. Absent the completion of regional climate change adaptation measures or significant changes to the MBTA system, our results suggest that even under more modest SLR projections (SSP1-2.6) expected increases in sea level will result in significant increases in coastal flood risk exposure for the MBTA in the short- and long-term. Under the most severe SLR condition

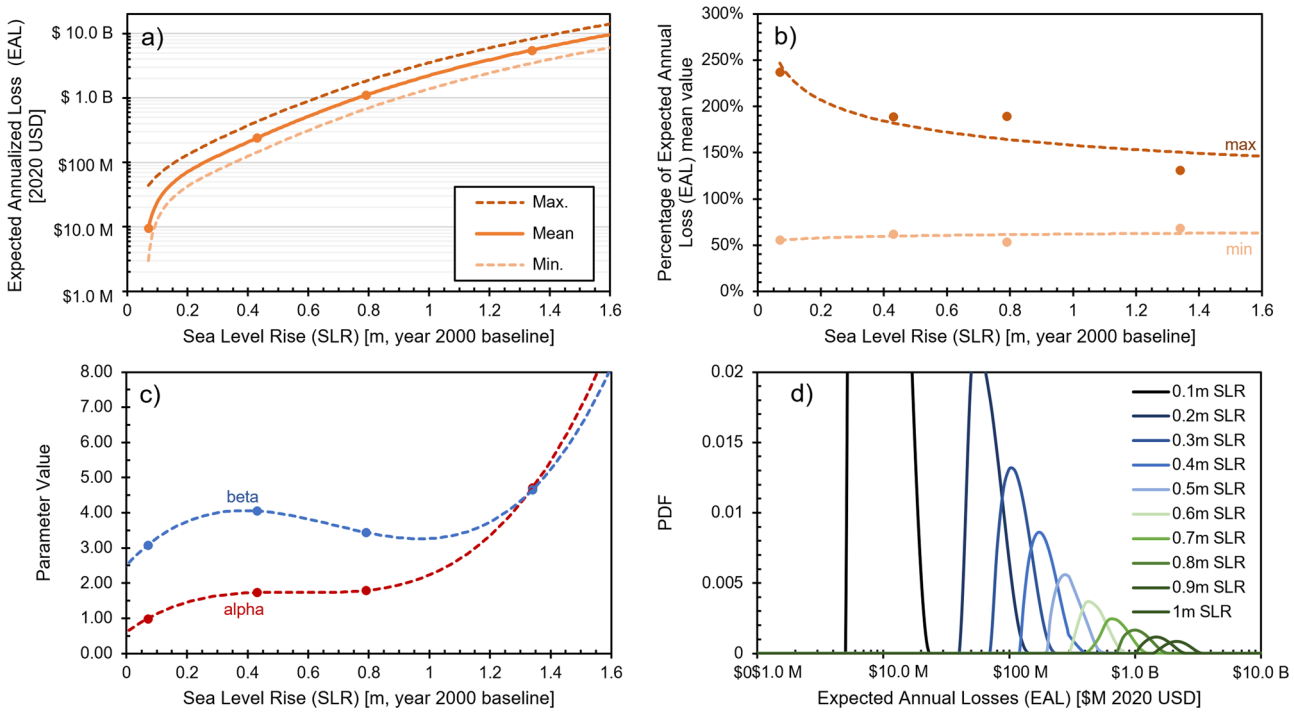

Fig. 4 MBTA rail rapid transit system Expected Annual Loss (EAL) characteristics. a Min (light orange dashed line), mean (orange solid line and data points), and max (dark orange dashed line) EAL vs. sea level rise (SLR). **b** Min (light orange) and max (dark orange) EAL as a percentage of EAL mean value. **c** generalized beta distribution parameter values (alpha parameter in red, beta parameter in blue) vs. SLR. **d** EAL probability density functions for several sample SLR values (color gradient from navy blue to forest green for increasing SLR values).

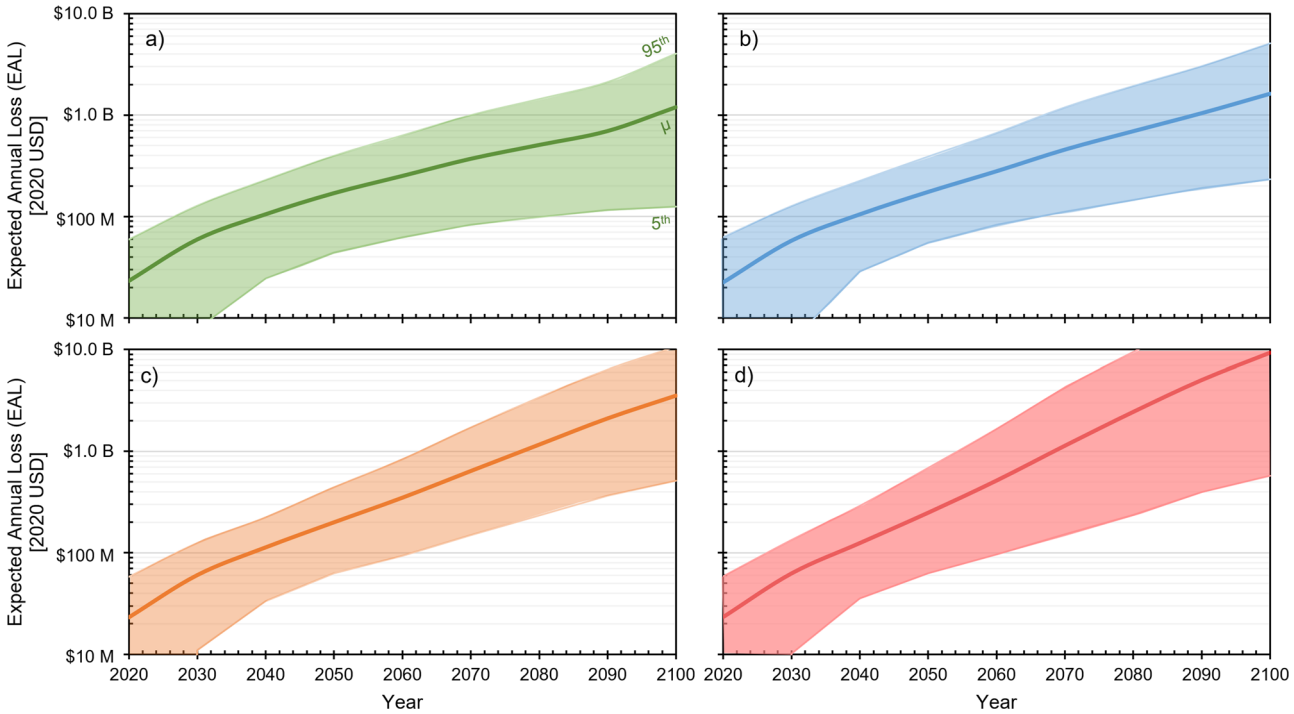

Fig. 5 MBTA rail rapid transit system Expected Annual Losses (EAL) associated with coastal flood risk over time under several uncertain IPCC 6th Assessment Report (AR6) sea level rise (SLR) projections. Expected values (thick line) and 90% confidence interval (shaded regions) for uncertain EAL over time, given uncertain future SLR projections under the: **a** SSP1-2.6 projection (green), **b** SSP2-4.5 projection (blue), **c** SSP5-8.5 (orange), **d** SSP5-8.5 projection inclusive of low confidence processes (red).

assessed (+1.34 m), which is entirely plausible by the end of this century according to several projections (SSP3-7.0, SSP5-8.5, SSP 5-8.5 low conf.[1,37–39]), we expect regular inundation of significant portions of the system absent any effective adaptation measures. Under the most severe SLR projection considered (SSP5-8.5 low confidence scenario) the $9.3B EAL expected in 2100 represents 96% of the MBTA's latest 5-year capital budget[41] and implies perpetual flood-related repairs and permanent service outages systemwide. While such an outcome is theoretically possible and clearly untenable, it would only occur in the complete absence of additional flood protection or climate adaptation measures. Though representative of a pessimistic future (i.e., in which no adaptation is undertaken through the end of the century), the analysis presented here provides a useful counterfactual that can establish a baseline expectation of future damages, which can serve as the basis for quantification of flood risk reduction benefits of future adaptation projects.

The analysis framework (including the data collection it necessitates) and subsequent results can also directly inform climate adaptation measures and help prioritize flood risk reduction efforts throughout the system. The cataloging of lowest critical locations (LCLs), a crucial step in the analysis presented, can provide transit agencies with a comprehensive list of locations where flood risk mitigation measures are likely needed. Taken together with the results provided by coupled hydrodynamic and hydraulic analysis presented above, planners and decision makers can better understand which LCLs are most exposed to coastal flooding and the consequent inflow volumes, damage costs, etc.

Within this case study, Aquarium Station (Fig. 1; ~+2.5 m NAVD88) is likely the first location to experience coastal flooding, as other LCLs at comparable or lower elevations (i.e., most tunnel portals, Central Square Station, Kendall/MIT Station, and Alewife Station) are either situated behind dams (e.g., Kendall/MIT Station on the Red Line lies behind the New Charles River dam) or surrounded by comparatively higher ground (e.g., the Airport Portal on the Blue Line). Although Aquarium Station is likely the first location to experience inundation during a coastal flood event, the consequences of flood exposure at tunnel portal locations are disproportionately severe, as they allow much larger inflows into the underground portions of the system, due in part to their comparatively low invert elevations and largely unobstructed open channel flow. Taken together, these results suggest that providing flood risk reduction measures at Aquarium Station and at tunnel portal locations should be the top priority.

The extent of flooding under certain scenarios (e.g., the 1-in-2-year coastal flood with +1.34 m SLR; Supplementary Fig. 18) demonstrates that interconnected portions of the underground network are sufficiently well connected hydraulically at interconnecting stations to allow floodwaters to flow between transit lines. This result is significant, as it suggests that absent a uniform level of protection at all LCLs connected to the central tunnel network, sufficient inflow at a single unprotected LCL (tunnel portals in particular) could nonetheless result in significant inundation of the central tunnel network, thereby negating the benefits of protection at other locations. This has significant and practical implications for transit infrastructure managers, highlighting that flood risk mitigation measures for the central tunnel network must be designed as a system to provide uniform protection across all LCLs to ensure their effectiveness. Given their outsized contribution to flood ingress, the protection of tunnel portals should be afforded a high priority, particularly compared to protection of at-grade portions of the rail rapid transit system.

When considering such investments in longer-term flood risk reduction (i.e., climate change adaptation) projects, the analysis framework presented can allow for rapid prototyping and performance simulation of potential adaptation measures or regional flood protection projects, enabling planners to better quantify the benefits (i.e., avoided flood losses) of potential adaptation measures. Infrastructure managers can rely on these flood risk reduction benefits to make a clearer business case for investments in climate adaptation. Pricing risk provides a better justification for funding, either via established capital investment programs, or the introduction of new funding mechanisms, such as special assessment taxes, resilience fees, or green bonds[42–44]. In contrast to prior assessments, the asset-level model fidelity can also enable infrastructure managers to explore the implications at individual facilities or for separate subsystems (e.g., signal systems) thereby enabling discretization of risk and related adaptation priorities in a manner consistent with established organizational boundaries and allowing for more effective delegation of responsibility within a transit agency.

In addition to informing and estimating the value of adaptation planning efforts, the analysis framework and results presented can inform and support the structuring of near-term, risk transfer strategies. Near-term estimates of flood damage costs for a particular coastal flood event (e.g., 1-in-100-year) or expected annualized losses can aid transit agencies in the pricing and negotiation of risk transfer measures, such as conventional indemnity-based insurance policies or less conventional risk transfer strategies, such as the issuance of parametric catastrophe bonds or resilience bonds[43,44]. The analysis framework presented can enable insurers and transit agencies to devise infrastructure-specific parametric policy triggers, while also enabling more effective pricing of subsequent payouts for parametric insurance policies or catastrophe bonds.

While the coastal flood loss projections presented are undoubtedly significant, they likely represent an underestimate of overall costs. In an event where there is significant and widespread damage to the transit network, system restoration and repair costs are liable to be subject to macroeconomic forcings that could significantly increase overall repair costs (e.g., supply chain or labor availability constraints[32,45,46]. Furthermore, the analysis presented here assumes that infrastructure managers will opt to fully repair assets or replace in-kind, rather than upgrading with more modern or expensive equipment. In addition to the direct damage costs to infrastructure quantified in this research, there are significant indirect costs associated with system disruption, which are not quantified in this study. Loss of access to public transport will disrupt travel and impose significant adverse economic consequences on passengers[47,48], business interruption (i.e., loss of farebox revenue), and losses associated with regional economic disruption[49]. Conversely, budgetary and finance constraints may force infrastructure managers to defer fixing flood-related damages, nominally reducing flood damage costs by shifting comparatively less urgent repairs (e.g., deterioration of tunnel bench walls[50]) into a maintenance backlog, potentially deferring repairs for several years[50]. If faced with significant and widespread damage and an inadequate availability of capital, infrastructure managers may be forced to abandon damaged infrastructure and alter service patterns, in effect making an involuntary but managed retreat which would undoubtedly have significant implications for the adjacent built environment and socioeconomic system[51].

Though the analysis presented only considers coastal flood risk, the framework is readily extensible to consider other sources of flooding (i.e., pluvial or fluvial flooding) or compound flood hazards, should sufficient data be readily available to adequately characterize expected future regional nonstationarity in these additional flood sources for as full of a range as possible. Further, the analysis framework presented can also enable consideration of SLR-induced increases in groundwater levels[52], which based on conventional analytical methods[53] would lead to higher rates of

groundwater infiltration into tunnels. Additionally, the analysis framework presented is readily extensible to other types of infrastructure systems (e.g., roadway networks, pipelines, regional electric grids, etc.) assuming sufficient information characterizing asset-level coastal flood fragility (i.e., asset-specific depth damage curves) are readily available for relevant assets and subsystems.

Rail rapid transit systems in coastal cities are likely already experiencing significant increases in coastal flood risk. The proposed analysis framework can enable infrastructure managers to understand the direct damage consequences associated with more severe coastal flood events under future SLR conditions and quantify how coastal flood risk exposure is increasing over time. We demonstrate coastal flood risk to the MBTA rail rapid transit system, as measured by expected annualized losses (EAL), has already more than doubled since 2008 and is expected to double again by 2030 if no adaptation or flood risk reduction measures are undertaken. Even in the short-term, failure to adapt will cause unacceptable levels of coastal flood risk. Adequately planning for rapidly increasing coastal flood risk requires an understanding of where water can flow into underground portions of a transit network, as well as an understanding of how water can flow between interconnected underground portions of the network. Our results suggest that in the absence of effective adaptation and flood risk reduction measures at all flood ingress pathways, interconnected underground portions of a network can still experience significant flooding. Through modeling coastal flood exposure and quantifying resulting direct damage costs and expected annualized losses, transit infrastructure managers can better plan adaptation projects, directly quantify their flood risk reduction benefits, and establish a clear business case for specific and actionable investments in climate adaptation.

Methods

Quantification of coastal flood damage costs requires a detailed understanding of coastal flood risk exposure, as well as an understanding of how exposure severity is expected to change with future SLR. Here, we rely on prior hydrodynamic simulation data provided by the Massachusetts Coastal Flood Risk Model (MC-FRM[31]) to characterize coastal flood risk exposure for a variety of coastal flood events of varying severity for several SLR regimes. An extension of the earlier Boston Harbor Flood Risk Model (BH-FRM[54]), the MC-FRM covers a wider area at higher spatial resolution (up to 3 m). Both the BH-FRM and MC-FRM simulate a suite of synthetic tropical and extra tropical storms (calibrated to present and expected future storm severities) to characterize the full range of potential coastal flood events impacting Massachusetts[54]. Each simulation run dynamically simulates a variety of physical processes, considering tides, currents, wind shear-induced storm surge, near-shore waves, wave run up and overtopping to fully characterize coastal flood risk[31,54]. The MC-FRM characterizes flood risk across 4 SLR regimes (+0.07 m; a 2008 baseline, +0.43 m, +0.79 m, +1.34 m; relative to year 2000 baseline). These particular SLR conditions represent the upper bound (99.5th percentile) of worst case SLR projections (RCP8.5[55]) in alignment with policy set by the Massachusetts office of Coastal Zone Management[31]. For the purposes of this analysis, we assess flood exposure and damage costs for the 1-in-2-year (50% coastal flood exceedance probability; CFEP), 1-in-10-year (10% CFEP), 1-in-20-year (5% CFEP), 1-in-100-year (1% CFEP), and 1-in-1000-year (0.1% CFEP) flood events for each SLR regime. For each coastal flood event, the MC-FRM provides flood depths, as well as water surface elevations over time for a set of 30 hydraulically distinct regions of the model domain. This coastal flood event catalog serves as the basis of the flood damage cost estimation model, as shown in Fig. 6.

Next, we construct a hydraulic model of the underground portions of the MBTA rail rapid transit system using EPA Storm Water Management Model (SWMM 5.1; hereafter referred to as SWMM). While SWMM is typically used to analyze precipitation runoff and design storm water drainage infrastructure systems, as the name implies, a key function of the software is the simulation of 1-Dimensional flow through pipe networks in discrete time. SWMM determines flow routing though a pipe network via the complete 1-D St Venant flow equations and calculates flow in individual pipes via the Manning equation[56].

We characterize the underground portions of the system via a set of junctions, $J = \{j_i \,|i = 1, 2, \ldots, J\}$ connected by a set of links, $L = \{l_k = (j_i, j_j)\,|k = 1, 2, \ldots, L;\ i, j = 1, 2, \ldots, J;\ i \neq j\}$. Each junction is characterized by an invert elevation, $E^J = \{e_i^J = |i = 1, 2, \ldots, J\}$ expressed relative to the North American Vertical Datum of 1988 (NAVD88) and a maximum depth, $D^J = \{d_i^J = |i = 1, 2, \ldots, J\}$. We obtain invert elevations from track geometry charts for each transit line (internal MBTA documentation), selecting junction locations as the boundaries of underground stations and at changes in track slope (i.e., points of vertical intersection, PVI, along the vertical track alignment). Links are further described by a length, $\Lambda^L = \{\lambda_k^L\,|k = 1, 2, \ldots, L\}$ also obtained directly from track alignment charts, and a tunnel cross-section as provided the MBTA tunnel inspection manual (internal documentation). We consider each rapid transit line tunnel as a separate series of connected links. Hydraulic interconnections at connecting (i.e., transfer) stations are modeled via inclusion of a separate link, whose length and cross section are informed by the total number of interconnections (i.e., staircases, elevator shafts, multi-level mechanical rooms) between connecting transit lines at the station as identified in as-built construction drawings (internal MBTA documentation). In addition to the main interconnected underground portions of the system in Downtown Boston, we model the Red Line tunnels in Cambridge and Dorchester as independent tunnel sections in the analysis. Lastly, based on expert judgment and discussion with the MBTA, we neglect the presence of existing tunnel pumps (primarily designed for groundwater infiltration), as there is insufficient information to adequately characterize their comparatively minimal capacity.

For each flood event within the event catalog (i.e., for $n = 20$ coastal flood events), we develop a set of flood depths throughout the rail rapid transit system via a systemwide flood model. We first sample MC-FRM provided flood depths along the at-grade portions of the system at a set of system sample locations (SSL) where available, extrapolating flood depths as needed based on available data and expected generalize extreme value (GEV) distributions describing extreme sea level in Boston Harbor[40] modulating the location parameter where necessary to adjust for SLR[2]. SSLs were placed at either end of at-grade station platforms, bridges, or underpasses. Each SSL was assigned an ID, associated with a transit line, and assigned a longitudinal station consistent with internal MBTA track alignment data (Supplementary Table 1). Next, assessing coastal flood exposure for the underground portions of the system, we obtain water surface elevation time series data for each lowest critical location (LCL[57]) in the system. For each LCL (Supplementary Table 2), given its estimated elevation (provided by publicly available data[58]) its dimensions, and hydraulic characteristics, we calculate inflow for each time step provided using standard hydraulics equations[59]:

$$Q_{LCL}(t) = \begin{cases} 3.33\left(w_{LCL} - 0.2\left(h_{LCL}(t) - z_{LCL}\right)\right)\left(h_{LCL}(t) - z_{LCL}\right)^{\frac{3}{2}} & \textit{if weir} \\ 0.2 w_{LCL}^2 \sqrt{2g\left(h_{LCL}(t) - z_{LCL}\right)} & \textit{if orifice} \\ \frac{1.49}{n}\left(w_{LCL} h_{LCL}(t)\right)\left(w_{LCL} + 2h_{LCL}(t)\right)^{\frac{2}{3}} S_{LCL}^{\frac{1}{2}} & \textit{if open channel} \end{cases} \quad (1)$$

Where $h_{LCL}(t)$ denotes the water surface elevation at time step t, w_{LCL} denotes the characteristic hydraulic width of the LCL, S_{LCL} denotes the slope of the LCL in instances of open channel flow, and n denotes the Manning's roughness coefficient. We then sum the inflows of geospatially adjacent LCLs and assign the resulting inflow time series as input into a hydraulic model of the underground portions of the transit system constructed in EPA SWMM 5.1[56]. The resulting underground and at-grade flood depths are used to define a water surface elevation for each rail rapid transit line; top of rail and tunnel crowns elevations are used to determine flood depths at a 3 m interval along each line, at the boundaries of station platforms, and locations of rail maintenance facilities.

Next, given these flood extents for a flood event of interest, in the cost estimation model, we generate probabilistic estimates via Monte Carlo simulation, repeatedly estimating flood damage costs by stochastically sampling uncertain variables to generate a large sample ($n = 10{,}000$ trials) of flood damage cost estimates. In each trial, flood losses are estimated via the unit loss method[6], where the overall damage cost, C_D, is defined as:

$$C_D = \sum_{i=1}^{N} R_i f_{dd_i}(d_i) \quad (2)$$

Where R_i is the sampled uncertain replacement cost of unit i, d_i is the sampled uncertain flood depth at unit i, $f_{dd_i}(d_i)$ the sampled uncertain depth-damage factor for unit i given its depth of flooding, and N is the total number of units in the study area. Here, we discretize linear assets into 3 meter increments (rail, signals, power, lighting, tunnel structure) and consider individual facilities (stations, maintenance yards) as separate analysis units. We generate uncertain replacement cost estimates via a two-step process. First, where available, we obtain point estimates of replacement costs for all assets from internal MBTA documentation and publicly available bid comparison and capital investment reports[60–64]. Replacement cost estimates were reviewed via interviews with MBTA personnel and escalated to 2020 price levels where appropriate. Second, these point estimates are converted to an uncertain (i.e., probabilistic) replacement cost estimates by applying an uncertain contingency factor calibrated to real-world variability in rail project costs[35], consistent with best practice recommendations for early-stage cost contingency estimation[65]. Consequently, we assume replacement cost estimates follow a normal distribution $N(1.45C_{est}, 0.38C_{est})$ wherein C_{est} denotes the point estimate replacement cost for a given asset of interest. Supplementary Tables 3 and 4 provide the replacement cost point estimates and uncertain replacement cost estimates employed in analysis.

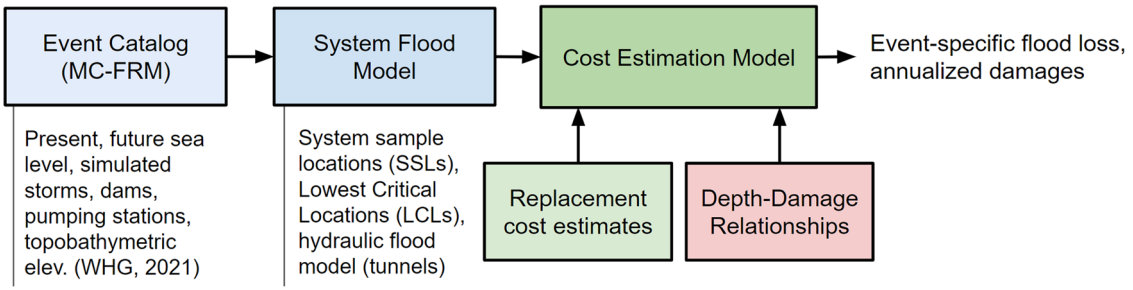

Fig. 6 Schematic representation of flood damage cost estimation model. A catalog of coastal flood events (light blue) from the Massachusetts Coastal Flood Risk Model[54] informs the system flood model (blue). This model, along with replacement cost estimates (light green) and depth-damage relationships (light red) inform the flood damage cost estimation model (green), which enables estimation of event-specific flood losses and annualized damages.

Uncertain depth-damage factors for each asset type are generated via a similar two-step process. For each asst type, we first establish an expected depth-damage curve, applying the transit-specific saltwater depth-damage functions provided by Martello et al.[32]. Next, variability and uncertainty in the depth-damage relationship is characterized by the method outlined by Egorova et al.[36]. In this method, an uncertain depth-damage function is generated via a beta distribution (i.e., $f_{dd}(d) = \beta(\alpha(d), \beta(d))$) informed by an expected (i.e., mean) depth-damage relationship, $f^*_{dd}(d)$, and an uncertainty parameter, $k = 0.4$, characterizing the variability in outcomes at a given depth, d. The beta distribution parameters, $\alpha(d)$ and $\beta(d)$, are defined as:

$$\alpha(d) = \left(\frac{1}{k} - 1\right) f^*_{dd}(d) \tag{3}$$

$$\beta(d) = \left(\frac{1}{k} - 1\right)\left(1 - f^*_{dd}(d)\right) \tag{4}$$

Finally, in alignment with prior work[34,66] to acknowledge uncertainty in estimated flood depths for a given scenario, we consider flood depth uncertainty for each analysis unit via a normal distribution, $d = N(d_{est}, 0.122 d_{est})$, where d_{est} denotes the estimated flood depth at the analysis unit of interest.

For each coastal flood event, after all trials are complete, we develop summary statistics (i.e., min, max, mean, variance) characterizing overall flood loss estimates, as well as those for each line, flooded facility, and linear asset class (summarized both systemwide and for each transit line). Cost breakdown probability distributions are approximated via generalized beta distributions based on sample distribution summary statistics[67]. Expected annualized losses (EAL) are found by computing the area under the flood loss vs. CFEP curve:

$$EAL = \int_0^1 f_B(p)dp \tag{5}$$

where $f_B(p)$ denotes the flood damage cost for a given coastal flood exceedance probability (CFEP), p. Using this equation, we compute EAL using the mean, minimum, and maximum flood loss estimates obtained from the flood damage cost estimation model. Here, we develop continuous closed-form function to describe how the mean and variance of EAL values varies with SLR via polynomial regression. We also characterize how the minimum and maximum EAL values (expressed as a percentage of mean EAL values) varies with SLR via a power law regression. This enables direct characterization of how uncertain EAL estimates are expected to change with respect to SLR, though is insufficient for characterizing EAL over time, as any such characterization requires selection of a SLR projection.

To develop estimates of how EAL changes over time, we apply a separate Monte Carlo simulation-based approach, considering uncertainty in EAL and SLR. First, we characterize the uncertainty in EAL with respect to SLR value via a generalized beta distribution, $EAL_{SLR}\beta(\alpha, \beta, EAL_{\min}(SLR), EAL_{\max}(SLR))$, wherein:

$$\alpha = \frac{EAL_{mean}(SLR) - EAL_{\min}(SLR)}{EAL_{\max}(SLR) - EAL_{\min}(SLR)} \left(\frac{\frac{EAL_{mean}(SLR) - EAL_{\min}(SLR)}{EAL_{\max}(SLR) - EAL_{\min}(SLR)} \left(1 - \frac{EAL_{mean}(SLR) - EAL_{\min}(SLR)}{EAL_{\max}(SLR) - EAL_{\min}(SLR)}\right)}{\left(\frac{EAL_{var}(SLR)^2}{(EAL_{\max}(SLR) - EAL_{\min}(SLR))^2}\right)^2} - 1 \right) \tag{6}$$

$$\beta = \frac{\alpha}{\frac{EAL_{mean}(SLR) - EAL_{\min}(SLR)}{EAL_{\max}(SLR) - EAL_{\min}(SLR)}} - \alpha \tag{7}$$

α and β are shape parameters, $EAL_{\min}(SLR)$, $EAL_{\max}(SLR)$, $EAL_{mean}(SLR)$, $EAL_{\text{var}}(SLR)$ are the EAL minimum, maximum, mean, and variance for the SLR value of interest. Characterizing EAL uncertainty in this manner (i.e., defining a probability distribution via a set of closed-form functions) enables development of EAL uncertainty for any SLR value. Using this characterization of EAL uncertainty and a subset of available SLR projections for Boston Harbor provided by the IPCC[1,37–39] as shown in Supplementary Fig. 2, we estimate EAL through 2100 on a $t = 10$-year interval. For each year of interest, we generate $n = 10{,}000$ EAL values by first generating a SLR sample, then developing and sampling the associated EAL probability distribution.

Data availability

A portion of the data supporting the findings of this study is subject to a non-disclosure agreement and cannot be made publicly available. The remaining data that support the findings of this study are publicly available at: https://doi.org/10.5281/zenodo.7764881. The datasets used to generate figures presented in this study are available at: https://doi.org/10.6084/m9.figshare.22329079.

Code availability

The models and code that support the findings of this study are publicly available at: https://doi.org/10.5281/zenodo.7764881.

Received: 5 September 2022; Accepted: 14 April 2023;
Published online: 24 April 2023

References

1. Intergovernmental Panel on Climate Change (IPCC). *Climate Change 2022: Impacts, Adaptation, and Vulnerability*. Contribution of Working Group II to the Sixth Assessment Report of the Intergovernmental Panel on Climate Change (Cambridge University Press, 2022).
2. Sweet, W. V. et al. *Global and Regional Sea Level Rise Scenarios for the United States: Updated Mean Projections and Extreme Water Level Probabilities Along U.S. Coastlines. NOAA Technical Report NOS 01* (National Oceanic and Atmospheric Administration, National Ocean Service, 2022). https://oceanservice.noaa.gov/hazards/sealevelrise/noaa-nostechrpt01-global-regional-SLR-scenarios-US.pdf.
3. Hallegatte, S., Green, C., Nicholls, R. J. & Corfee-Morlot, J. Future flood losses in major coastal cities. *Nat. Clim. Change* **3**, 802–806 (2013).
4. Strauss, B. H. et al. Economic damages from Hurricane Sandy attributable to sea level rise caused by anthropogenic climate change. *Nat. Commun.* **12**, 2720 (2021).
5. United States Army Corps of Engineers (USACE). *Catalog of Residential Depth-Damage Functions Used by the Army Corps of Engineers in Flood Damage Estimation. IWR Report 92-R-3*. https://www.iwr.usace.army.mil/Portals/70/docs/iwrreports/92-R-3.pdf (1992).
6. de Moel, H. *Uncertainty in Flood Risk*. PhD Thesis (VU University Amsterdam, 2012) https://research.vu.nl/ws/portalfiles/portal/42215325/complete+dissertation.pdf.
7. United States Army Corps of Engineers (USACE). *HEC-FDA Flood Damage Reduction Analysis – User's Manual*. Report CPD-72 Version 1.4.1. (USACE, 2016) https://www.hec.usace.army.mil/software/hec-fda/documentation/CPD-72_V1.4.1.pdf.
8. Federal Emergency Management Agency (FEMA). *Hazus Flood Model User Guide – Hazus 5.1* (FEMA, 2022) https://www.fema.gov/sites/default/files/documents/fema_hazus-5.1-flood-model-user-guidance.pdf.
9. United States Army Corps of Engineers (USACE). *New York-New Jersey Harbor and Tributaries Study (HATS) Coastal Storm Risk Management Feasibility Study: Draft Integrated Feasibility Report and Teir 1 Environmental Impact Statement* (USACE, 2022). https://www.nan.usace.army.mil/Portals/

37/NYNJHATS%20Draft%20Integrated%20Feasibility%20Report%20Tier%201%20EIS_1.pdf.
10. Gerl, T., Kreibich, H., Franco, G., Marechal, D. & Schröter, K. A review of flood loss models as basis for harmonization and benchmarking. *PLOS One* **11**, e0159791 (2016).
11. Franco, G., Becker, J. F. & Arguimbau, N. Evaluation methods of flood risk models in the (re)insurance industry. *Water Security* **11**, 100069 (2020).
12. Oddo, P. C. et al. Deep uncertainties in sea-level rise and storm surge projections: Implications for coastal flood risk management. *Risk Anal.* **40**, 153–168 (2020).
13. Rasmussen, D. J., Buchanan, M. K., Kopp, R. E., & Oppenheimer, M. A flood damage allowance framework for coastal protection with deep uncertainty in sea level rise. *Earths Future*, **8**, (2020). https://doi.org/10.1029/2019EF001340.
14. Aerts, J. C. J. H., Botzen, W. J. W., de Moel, H. & Bowman, M. Cost estimates for flood resilience and protection strategies in New York City: Flood management strategies for New York City. *Ann. N.Y. Acad. Sci.* **1294**, 1–104 (2013).
15. Hallegatte, S. et al. Assessing climate change impacts, sea level rise and storm surge risk in port cities: a case study on Copenhagen. *Clim. Change* **104**, 113–137 (2011).
16. De Moel, H. & Aerts, J. C. J. H. Effect of uncertainty in land use, damage models and inundation depth on flood damage estimates. *Nat. Hazards* **58**, 407–425 (2011).
17. Jacob, K., Rosenzweig, C., Horton, R., Major, D., & Gornitz, V. *MTA Adaptations to Climate Change: A Categorical Imperative* (Metopolitan Transportation Authority (MTA), 2008). https://new.mta.info/document/10451.
18. Martello, M. V., Whittle, A. J., Keenan, J. M. & Salvucci, F. P. Evaluation of climate change resilience for Boston's rail rapid transit network. *Transp. Res. Part D Transp. Environ.* **97**, 102908 (2021).
19. Kellermann, P., Schönberger, C. & Thieken, A. H. Large-scale application of the flood damage model Railway **I**nfrastructure **L**oss (RAIL). *Nat. Hazards Earth Syst. Sci.* **16**, 2357–2371 (2016).
20. Bubeck, P. et al. Global warming to increase flood risk on European railways. *Clim. Change* **155**, 19–36 (2019).
21. Sun, H., Li, M., Jiang, H., Ruan, X. & Shou, W. Inundation resilience analysis of metro-network from a complex system perspective using the grid hydrodynamic model and FBWM approach: a case study of Wuhan. *Remote Sens.* **14**, 3451 (2022).
22. Compton, K. L. (ed.) *Uncertainty and Disaster Risk Management: Modeling the Flash Flood Risk to Vienna and Its Subway system* (IIASA, 2009).
23. Sun, D., Wang, H., Lall, U., Huang, J. & Liu, G. Subway travel risk evaluation during flood events based on smart card data. *Geomat. Nat. Hazards Risk* **13**, 2796–2818 (2022).
24. Forero-Ortiz, E., Martínez-Gomariz, E. & Cañas Porcuna, M. A review of flood impact assessment approaches for underground infrastructures in urban areas: a focus on transport systems. *Hydrol. Sci. J.* **65**, 1943–1955 (2020).
25. Wang, G. et al. Flood risk assessment of subway systems in metropolitan areas under land subsidence scenario: a case study of Beijing. *Remote Sens.* **13**, 637 (2021).
26. Rosenzweig, C., et al. (eds). *Responding to Climate Change in New York State: The ClimAID Integrated Assessment for Effective Climate Change Adaptation*. Technical Report. (New York State Energy Research and Development Authority (NYSERDA), 2011). www.nyserda.ny.gov.
27. Terada, M., Ishigaki, T., Ozaki, T., Baba, Y., & Toda, K. Subway Inundation by Fluvial Flooding and Evacuation from Subway Stations. In *Proceedings of the 37th IAHR World Congress* (IAHR World Congress, 2017).
28. Massachusetts Bay Transportation Authority (MBTA). *ENVPS04 – Task Order No. 1 – Climate Change Vulnerability Assessment & Adaptation Flood Model Report – MBTA Blue Line – Aquarium Station to Maverick Portal* (Weston & Sampson and Arup., 2019).
29. Forero-Ortiz, E., Martínez-Gomariz, E., Cañas Porcuna, M., Locatelli, L. & Russo, B. Flood risk assessment in an underground railway system under the impact of climate change—a case study of the Barcelona Metro. *Sustainability* **12**, 5291 (2020).
30. Miura, Y. et al. A methodological framework for determining an optimal coastal protection strategy against storm surges and sea level rise. *Nat. Hazards* **107**, 1821–1843 (2021).
31. Woods Hole Group (WHG). (2021, Oct.). *Massachusetts coastal flood risk model time series water surface elevations*. [dataset]. Woods Hole Group (WHG), 2021).
32. Martello, M. V., Whittle, A. J., & Lyons-Galante, H. R. Depth-damage curves for rail rapid transit infrastructure. *J. Flood Risk Manag.* https://doi.org/10.1111/jfr3.12856 (2023).
33. Wagenaar, D. J., de Bruijn, K. M., Bouwer, L. M. & de Moel, H. Uncertainty in flood damage estimates and its potential effect on investment decisions. *Nat. Hazards Earth Syst. Sci.* **16**, 1–14 (2016).
34. Prahl, B. F., Rybski, D., Boettle, M. & Kropp, J. P. Damage functions for climate-related hazards: unification and uncertainty analysis. *Nat. Hazards Earth Syst. Sci.* **16**, 1189–1203 (2016).
35. Flyvbjerg, B., Holm, M. S. & Buhl, S. Underestimating costs in public works projects: error or lie? *J. Am. Plan. Assoc.* **68**, 279–295 (2002).
36. Egorova, R., van Noortwijk, J. M. & Holterman, S. R. Uncertainty in flood damage estimation. *Int. J. River Basin Manag.* **6**, 139–148 (2008).
37. Fox-Kemper, B. et al. Ocean, cryosphere and sea level change. In: *Climate Change 2021: The Physical Science Basis. Contribution of Working Group I to the Sixth Assessment Report of the Intergovernmental Panel on Climate Change* (eds Masson-Delmotte, V., et al.) (Cambridge University Press, 2021).
38. Garner, G. G. et al. *IPCC AR6 Sea Level Projections* (Version 20210809) [Data set]. (Zenodo, 2021a). https://doi.org/10.5281/ZENODO.5914709.
39. Garner, G. G. et al. *IPCC AR6 Sea-Level Rise Projections* (Version 20210809) [Data set]. (PO.DAAC, 2021b). https://podaac.jpl.nasa.gov/announcements/2021-08-09-Sea-level-projections-from-the-IPCC-6th-Assessment-Report.
40. NOAA. *Boston, MA – Station ID: 8443970*. https://tidesandcurrents.noaa.gov/stationhome.html?id=8443970 (2021).
41. Massachusetts Bay Transportation Authority (MBTA). *Massachusetts Bay Transportation Authority FY23-27 Capital Investment Plan (CIP) Proposed – March 2022* (MassDOT, 2022). https://cdn.mbta.com/sites/default/files/2022-03/2022-03-24-proposed-fy23-27-mbta-cip-2.pdf.
42. Levy, D. L., & Herst, R. *Financing Climate Resilience: Mobilizing Resources and Incentives to Protect Boston from Climate Risks* (Sustainable Solutions Lab, University of Massachusetts Boston, 2018). https://www.umb.edu/editor_uploads/images/centers_institutes/sustainable_solutions_lab/Financing_Climate_Resilience_April_2018.pdf.
43. Keenan, J. M. *Climate Adaptation Finance and Investment in California* (Routledge, Taylor & Francis Group, 2019).
44. Chen, C., & Bartle, J. R. *Innovative Infrastructure Finance: A Guide for State and Local Governments*. (Springer International Publishing, 2022). https://doi.org/10.1007/978-3-030-91411-0.
45. Olsen, A. H. & Porter, K. A. What we know about demand surge: brief summary. *Nat. Hazards Rev.* **12**, 62–71 (2011).
46. Golan, M. S., Trump, B. D., Cegan, J. C. & Linkov, I. Supply chain resilience for vaccines: Review of modeling approaches in the context of the COVID-19 pandemic. *Ind. Manag. Data Syst.* **121**, 1723–1748 (2021).
47. Suarez, P., Anderson, W., Mahal, V. & Lakshmanan, T. R. Impacts of flooding and climate change on urban transportation: a systemwide performance assessment of the Boston Metro Area. *Transp. Res. Part D Transp. Environ.* **10**, 231–244 (2005).
48. Sun, J., Chow, A. C. H. & Madanat, S. M. Equity concerns in transportation infrastructure protection against sea level rise. *Transp. Policy* **100**, 81–88 (2021).
49. National Academies of Sciences, Engineering, and Medicine (NASEM). *Incorporating the Costs and Benefits of Adaptation Measures in Preparation for Extreme Weather Events and Climate Change Guidebook* (p. 25744). (Transportation Research Board, National Oceanic and Atmospheric Administration, 2020). https://doi.org/10.17226/25744.
50. O'Rourke, T. D. Change agents for resilient infrastructure. In *2020 PEER Annual Meeting, UC Berkeley* (PEER, 2020).
51. Balboni, C. In harm's way? Infrastructure investments and the persistence of coastal cities. *Am. Econ. Rev.* https://economics.mit.edu/files/22033 (2021).
52. Hummel, M. A., Berry, M. S. & Stacey, M. T. Sea level rise impacts on wastewater treatment systems along the U.S. coasts. *Earths Future* **6**, 622–633 (2018).
53. Kong, W. K. Water ingress assessment for rock tunnels: a tool for risk planning. *Rock Mech. Rock Eng.* **44**, 755–765 (2011).
54. Bosma, K. et al. *MassDOT-FHWA Pilot Project Report: Climate Change and Extreme Weather Vulnerability Assessments and Adaptation Options for the Central Artery* (MassDOT, 2015). https://www.mass.gov/files/documents/2018/08/09/MassDOT_FHWA_Climate_Change_Vulnerability_1.pdf.
55. Kopp, R. E. et al. Evolving understanding of antarctic ice-sheet physics and ambiguity in probabilistic sea-level projections. *Earths Future* **5**, 1217–1233 (2017).
56. Rossman, L. A. *Storm Water Management Model User's Manual Version 5.1* (U.S. Environmental Protection Agency, National Risk Management Research Laboratory, 2015). https://www.epa.gov/sites/default/files/2019-02/documents/epaswmm5_1_manual_master_8-2-15.pdf.
57. Martello, M. V. *Resilience of Rapid Transit Networks in the Context of Climate Change*. Master's Thesis (Massachusetts Institute of Technology, 2020) https://dspace.mit.edu/handle/1721.1/127329.
58. United States Geological Survey (USGS). *The National Map (TNM) Elevation*. [dataset]. (United States Geological Survey (USGS), 2021) https://apps.nationalmap.gov/elevation/.
59. Finnemore, E. J., & Franzini, J. B. *Fluid mechanics with engineering applications* (10th ed.) (McGraw-Hill, 2009).

60. Massachusetts Bay Transportation Authority (MBTA). *Comparison of Bids: Contract R44CN01 – Red Line Test Track, South Boston, MA* (MassDOT, 2017) https://bc.mbta.com/business_center/bidding_solicitations/pdf/Bid%20Comparison%20Rpt%20-%20R44CN01.pdf.
61. Massachusetts Bay Transportation Authority (MBTA). *Comparison of Bids: Contract Q09CN02 – Green Line D Branch Trach & Signal Replacement-Beaconsfield to Riverside, Newton and Brookline* (MassDOT, 2018). https://old.mbta.com/business_center/bidding_solicitations/pdf/Bid%20Comparison%20Rpt%20-%20Q09CN02.pdf.
62. Massachusetts Bay Transportation Authority (MBTA). *Comparison of Bids: Contract B22CN02 – Repair/Rehabilitation of East Cambridge (Lechmere) Viaduct, Boston and Cambridge, MA* (MassDOT, 2019a). https://bc.mbta.com/business_center/bidding_solicitations/pdf/Bid%20Comparison%20Rpt%20-%20B22CN02.pdf.
63. Massachusetts Bay Transportation Authority (MBTA). *MBTA FY20-24 Capital Investment Plan: Evaluation Guide* (Massachusetts Department of Transportation, MassDOT, 2019c).
64. Massachusetts Bay Transportation Authority (MBTA). *Comparison of Bids: Contract A25CN01 – Green Line B Branch Station Consolidation, Boston, MA* (MassDOT, 2020). https://bc.mbta.com/business_center/bidding_solicitations/pdf/Bid%20Comparison%20Rpt%20-%20A25CN01.pdf.
65. Transportation Research Board (TRB) & National Academies of Sciences, Engineering, and Medicine (NASEM). *Guidance for Cost Estimation and Management for Highway Projects During Planning, Programming, and Preconstruction* (The National Academies Press, 2007). https://doi.org/10.17226/14014.
66. Saint-Geours, N., Grelot, F., Bailly, J.-S. & Lavergne, C. Ranking sources of uncertainty in flood damage modelling: a case study on the cost-benefit analysis of a flood mitigation project in the Orb Delta, France: Ranking sources of uncertainty in flood damage modelling. *J. Flood Risk Manag.* **8**, 161–176 (2015).
67. Guthrie, W. F. *NIST/SEMATECH e-Handbook of Statistical Methods (NIST Handbook 151)* [Data set]. (National Institute of Standards and Technology, 2020). https://doi.org/10.18434/M32189.

Acknowledgements

The research reported in this study was supported by the Massachusetts Bay Transportation Authority (MBTA) and the United States Department of Defense (via the DoD SMART Scholarship-for-Service Program). The opinions expressed in this paper are those of the Authors and do not represent those of the MBTA.

Author contributions

This study was conceptualized by A.J.W. and M.V.M. and supervised by A.J.W. Data collection, analysis, and initial manuscript preparation were performed by M.V.M. A.J.W. revised the manuscript and discussed results with M.V.M. at all stages. M.V.M. and A.J.W. revised the manuscript in response to reviewer comments.

Competing interests

The authors declare no competing interests.

Additional information

Supplementary information The online version contains supplementary material available at https://doi.org/10.1038/s43247-023-00804-7.

Correspondence and requests for materials should be addressed to Michael V. Martello.

Peer review information *Communications Earth & Environment* thanks Karl Kim, Jiayun Sun and the other, anonymous, reviewer(s) for their contribution to the peer review of this work. Primary Handling Editor: Joe Aslin. Peer reviewer reports are available.

Reprints and permission information is available at http://www.nature.com/reprints

Publisher's note Springer Nature remains neutral with regard to jurisdictional claims in published maps and institutional affiliations.

Terms and Conditions

Springer Nature journal content, brought to you courtesy of Springer Nature Customer Service Center GmbH (“Springer Nature”).
Springer Nature supports a reasonable amount of sharing of research papers by authors, subscribers and authorised users (“Users”), for small-scale personal, non-commercial use provided that all copyright, trade and service marks and other proprietary notices are maintained. By accessing, sharing, receiving or otherwise using the Springer Nature journal content you agree to these terms of use (“Terms”). For these purposes, Springer Nature considers academic use (by researchers and students) to be non-commercial.
These Terms are supplementary and will apply in addition to any applicable website terms and conditions, a relevant site licence or a personal subscription. These Terms will prevail over any conflict or ambiguity with regards to the relevant terms, a site licence or a personal subscription (to the extent of the conflict or ambiguity only). For Creative Commons-licensed articles, the terms of the Creative Commons license used will apply.
We collect and use personal data to provide access to the Springer Nature journal content. We may also use these personal data internally within ResearchGate and Springer Nature and as agreed share it, in an anonymised way, for purposes of tracking, analysis and reporting. We will not otherwise disclose your personal data outside the ResearchGate or the Springer Nature group of companies unless we have your permission as detailed in the Privacy Policy.
While Users may use the Springer Nature journal content for small scale, personal non-commercial use, it is important to note that Users may not:

1. use such content for the purpose of providing other users with access on a regular or large scale basis or as a means to circumvent access control;
2. use such content where to do so would be considered a criminal or statutory offence in any jurisdiction, or gives rise to civil liability, or is otherwise unlawful;
3. falsely or misleadingly imply or suggest endorsement, approval , sponsorship, or association unless explicitly agreed to by Springer Nature in writing;
4. use bots or other automated methods to access the content or redirect messages
5. override any security feature or exclusionary protocol; or
6. share the content in order to create substitute for Springer Nature products or services or a systematic database of Springer Nature journal content.

In line with the restriction against commercial use, Springer Nature does not permit the creation of a product or service that creates revenue, royalties, rent or income from our content or its inclusion as part of a paid for service or for other commercial gain. Springer Nature journal content cannot be used for inter-library loans and librarians may not upload Springer Nature journal content on a large scale into their, or any other, institutional repository.
These terms of use are reviewed regularly and may be amended at any time. Springer Nature is not obligated to publish any information or content on this website and may remove it or features or functionality at our sole discretion, at any time with or without notice. Springer Nature may revoke this licence to you at any time and remove access to any copies of the Springer Nature journal content which have been saved.
To the fullest extent permitted by law, Springer Nature makes no warranties, representations or guarantees to Users, either express or implied with respect to the Springer nature journal content and all parties disclaim and waive any implied warranties or warranties imposed by law, including merchantability or fitness for any particular purpose.
Please note that these rights do not automatically extend to content, data or other material published by Springer Nature that may be licensed from third parties.
If you would like to use or distribute our Springer Nature journal content to a wider audience or on a regular basis or in any other manner not expressly permitted by these Terms, please contact Springer Nature at

onlineservice@springernature.com